

1 **Full title:** Evaluation of CRISPR gene-editing tools in zebrafish

2 **Short title:** CRISPR gene-editing tools in zebrafish

3

4 José M. Uribe-Salazar^{1,2}, Aadithya Sekar¹, Gulhan Kaya¹, KaeChandra Weyenberg¹, Cole

5 Ingamells¹, Megan Y. Dennis^{1,2†}

6

7 ¹Genome Center, MIND Institute, and Department of Biochemistry & Molecular Medicine,

8 University of California, Davis, CA, USA; ²Integrative Genetics and Genomics Graduate Group,

9 University of California, Davis, CA, USA

10

11 [†]Corresponding author:

12 Megan Y. Dennis, Ph.D.

13 University of California, Davis, School of Medicine

14 One Shields Avenue

15 Genome Center, 4303 GBSF

16 Davis, CA 95616

17 Email: mydennis@ucdavis.edu

18

19 **Keywords:** *Danio rerio*, zebrafish, CRISPR, Cas9, gene knockout, CIRCLE-seq, RNA-seq.

1 ABSTRACT

2 Zebrafish have practical features that make them a useful model for higher-throughput tests of
3 gene function using CRISPR/Cas9 editing to create ‘knockout’ models. A large number of
4 computational and empirical tools exist to design CRISPR assays but often produce varied
5 predictions across methods. To systematically assess accuracy of tool predictions of on- and off-
6 target gene editing, we subjected zebrafish embryos to CRISPR/Cas9 with 50 different guide
7 RNAs (gRNAs) targeting 14 genes. We compared our experimental *in vivo* editing efficiencies in
8 mosaic G₀ embryos with those predicted by seven commonly used gRNA design tools and found
9 large discrepancies between methods. Assessing off-target mutations (predicted *in silico* and *in*
10 *vitro*) found that the majority of tested loci had low *in vivo* frequencies (<1%). To characterize if
11 commonly used ‘mock’ CRISPR controls (larvae injected with Cas9 enzyme or mRNA with no
12 gRNA) exhibited spurious molecular features that might exacerbate studies of G₀ mosaic
13 CRISPR knockout fish, we generated an RNA-seq dataset of various control larvae at 5 days post
14 fertilization. While we found no evidence of spontaneous somatic mutations of injected larvae,
15 we did identify several hundred differentially-expressed genes with high variability between
16 injection types. Network analyses of shared differentially-expressed genes in the ‘mock’ injected
17 larvae implicated a number of key regulators of common metabolic pathways, and gene-ontology
18 analysis revealed connections with response to wounding and cytoskeleton organization,
19 highlighting a potentially lasting effect from the microinjection process that requires further
20 investigation. Overall, our results provide a valuable resource for the zebrafish community for
21 the design and execution of CRISPR/Cas9 experiments.

1 BACKGROUND

2 Zebrafish (*Danio rerio*) are increasingly used to rapidly and robustly characterize gene functions
3 [1–4]. Features that make this model attractive over other classic vertebrate systems include
4 external fertilization, rapid development, a large number of progeny, embryonic transparency,
5 small size, and the availability of effective gene-editing tools [3, 5–12]. Continuous
6 improvements of CRISPR editing in zebrafish have allowed efficient targeting of multiple genes
7 simultaneously leading to rapid generation of either mosaic (G_0) or stable mutant lines and
8 subsequent characterizations of phenotypes [8, 13–19], which have been used to test candidate
9 genes associated with human diseases and developmental features [20]. The trend towards more
10 affordable higher-throughput protocols using zebrafish requires a careful evaluation of methods
11 used for the design of CRISPR-based genetic screens.

12

13 New and creative CRISPR-based approaches in zebrafish address biological questions related to
14 developmental processes (e.g., cell-lineage tracing) as well as gene functions (e.g., epigenome
15 editing and targeted mutagenesis, reviewed in [21]). In the latter application, important factors in
16 generating CRISPR gene knockouts include predicting/maximizing ‘on target’ Cas9 cleavage
17 activity, predicting/minimizing unintended ‘off-target’ editing events, and rapidly detecting
18 small insertions or deletions (indels). Presence of indels at candidate loci can be determined in an
19 affordable manner via a number of approaches (reviewed in [22]), ranging from simple
20 identification of heteroduplexes—arising from multiple alleles coexisting in the sampled DNA—
21 visualized using a polyacrylamide gel electrophoresis (PAGE) [23] to more sophisticated
22 sequencing approaches that precisely identify and quantify mutant alleles [14, 24]. On-target
23 activity of a particular guide RNA (gRNA) can be predicted using tools that provide efficiency

1 scores, often defined by information gathered across empirical assays [25]. One relevant example
2 is CRISPRScan, a predictive-scoring system built from experimental zebrafish gene-editing data
3 based on multiple factors such as nucleotide GC and AT content and nucleosome positioning [9,
4 26]. Bioinformatic tools also exist that define potential regions prone to off-target edits mainly
5 based on sequence similarity and the type/amount of mismatches relative to the on-target region
6 [26]. More recent empirical approaches couple *in vitro* cleavage of genomic DNA with Cas9
7 ribonucleoprotein, such as CIRCLE-seq [27] or GUIDE-seq [28], to provide a blind assessment
8 of editing sites but may not necessarily reflect the *in vivo* activity of the CRISPR/Cas9 complex.

9

10 Previous studies have shown CRISPR off-target activity *in vivo* to be relatively low in zebrafish
11 [8, 12, 18]. A cross-generational study identified no inflation of transmitted *de novo* single-
12 nucleotide mutations due to CRISPR-editing using exome sequencing and a stringent
13 bioinformatic pipeline [29] in a similar approach used to identify off-target mutations in mouse
14 trios [30, 31]. Other studies have observed off-target mutation rates ranging from 0.07 to 3.17%
15 in zebrafish by sequencing the top three to four predicted off-target regions based on sequence
16 homology [11, 12, 18]. Although off-target mutations should not significantly impact studies of
17 stable mutants, since unwanted mutations can be outcrossed out of studied lines relatively easily
18 [14, 21], they may be problematic in rapid genetic screens using G₀ mosaics that quickly test
19 gene functions in a single generation.

20

21 The increasing number of tools available for the design and execution of CRISPR screens
22 provide an important resource to the zebrafish community. Here, we assayed different available
23 CRISPR on- and off-target prediction methods using empirical data from Cas9-edited zebrafish

1 embryos. We quantified CRISPR cleavage efficiencies *in vivo* employing a variety of
2 experimental approaches and used these results to compare the accuracy of *in silico* and *in vitro*
3 tools for predicting Cas9 on- and/or off-target activity. Finally, we assayed G₀ ‘mock’ negative
4 control embryos injected with a buffer containing either Cas9 enzyme or mRNA in the absence
5 of gRNAs by performing RNA-seq and obtained a list of genes with significant differential
6 expression versus uninjected wild-type siblings. In all, these results will serve as a useful
7 resource to the research community as larger-scale CRISPR screens become more common in
8 assaying gene functions in zebrafish.

9

10 RESULTS

11 Identification of CRISPR-induced indels in zebrafish

12 We generated a dataset of experimentally confirmed indels within 14 protein-coding genes from
13 injected NHGRI-1 wild-type zebrafish larvae targeted by 50 gRNAs (2–4 different gRNAs/target
14 gene, assembled through the annealing of crRNA:tracrRNA) (Figure 1A, Supplementary Tables
15 1 and 2). To obtain experimental *in vivo* editing efficiency values for each gRNA, DNA
16 extracted from a pool of 20 G₀ mutant embryos —generated via microinjections of individual
17 gRNAs at the one-cell stage and harvested at five days post-fertilization (dpf)— was subjected to
18 PCR (~500 bp region) and Sanger sequencing of the gRNA predicted target site. From this, we
19 inferred an *in vivo* ‘efficiency score’ measured as the percentage of DNA from injected embryos
20 harboring indels compared to uninjected batch siblings. The percentage of indels was extracted
21 using two different tools that deconvolve major mutations and their frequencies within Sanger
22 traces —Tracking of Indels by DEcomposition (TIDE) [32] and Inference from CRISPR Edits
23 (ICE) [33] (Figure 1B). Briefly, these tools use the gRNA sequence to predict the cutting site in

1 the control trace, map the sample trace to this reference, identify indels by deconvolving all base
2 reads at each position, and provide a frequency of the indel spectrum [32, 33]. As previously
3 reported [33], both tools provided positively correlated *in vivo* scores across all gRNAs
4 (Spearman $\rho=0.87, p=6.78\times10^{-15}$) with an average score difference of 8.8 ± 12.1 between tools
5 (Figure 1C). We noted a higher correlation between tools in scores below the median (Spearman
6 $\rho=0.96, p=1.23\times10^{-13}$) than above the median (Spearman $\rho=0.65, p=0.00072$; Figure 1C),
7 suggesting that the deconvolution process in both tools is more accurate when fewer molecules
8 from the pool carry indels. To determine the more accurate tool, we performed Illumina
9 sequencing, which provides more precise molecular estimates of mosaicism, of ~200 bp PCR
10 fragments surrounding predicted cut sites for a subset of gRNAs (n= 6, each targeting a different
11 gene) with relatively high *in vivo* efficiencies (>50%). Using *CrispRVariants* [34] with
12 uninjected batch siblings DNA as reference, we extracted the proportion of reads carrying indel
13 alleles and identified a significant correlation with ICE (Spearman $\rho=0.93, p=0.0077$) but not
14 with TIDE (Spearman $\rho=0.08, p=0.919$, Figure 1D); we therefore moved forward with *in vivo*
15 efficiencies computed via the ICE tool. Additionally, we observed mosaicism quantified by
16 Illumina to be 23.6 ± 4.3 higher versus ICE editing scores, suggesting the Sanger sequencing tool
17 underestimates mosaicism for gRNAs with higher editing efficiencies (Figure 1D).

18
19 A quicker and more affordable approach to quantify CRISPR cleavage efficiency is via PAGE,
20 which takes advantage of the heteroduplexes produced from DNA harboring a mosaic mix of
21 different types of indel mutations [23]. We performed PAGE on ~200 bp regions surrounding the
22 predicted target site for each gRNA and quantified the PCR ‘smear’ intensity ratio of injected
23 versus uninjected controls (see Methods). These intensity ratios were weakly correlated with our

1 *in vivo* efficiency scores (Spearman $\rho=0.38$, $p=0.0179$; Figure 1E) indicating that accurate
2 quantitative efficiencies cannot be directly deduced from PAGE but that the intensity of PCR
3 ‘smear’ does qualitatively convey CRISPR-cleavage efficiency.

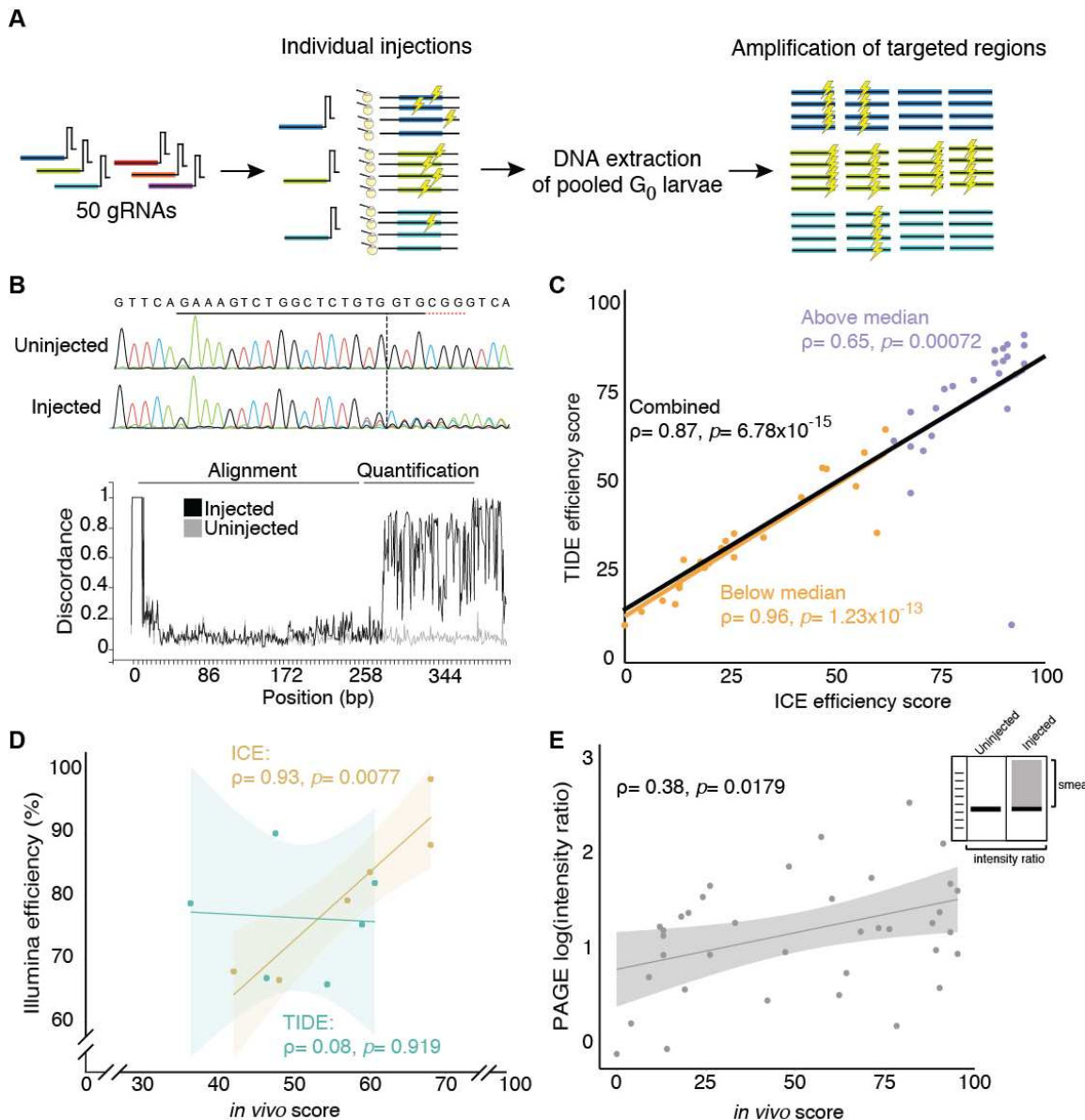


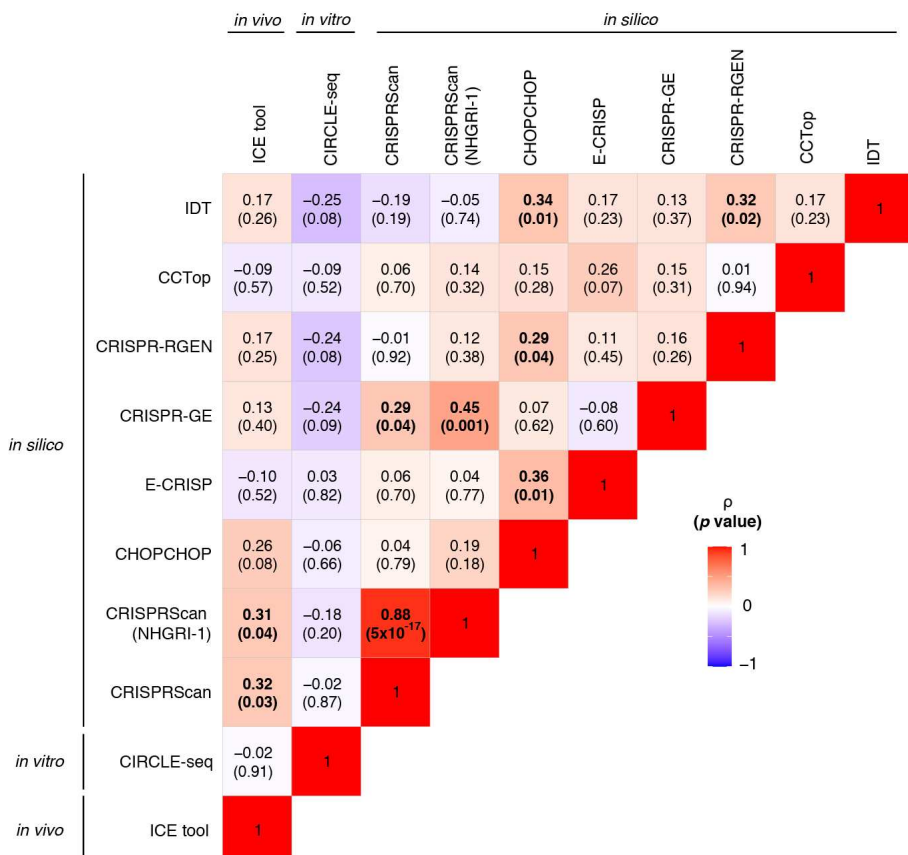
Figure 1. Workflow for the evaluation of CRISPR cleavages in NHGRI-1 zebrafish embryos. (A) The cartoon depicts our experiment, which included 50 gRNAs individually microinjected into one-cell stage embryos, DNA extracted from 20 pooled G₀ larvae, and genomic regions targeted by the gRNA amplified. Cartoon lightning symbols represent a cleavage event. (B) An *in vivo* score was obtained from the Sanger sequencing traces using the ICE and TIDE tools, with an example output from ICE pictured. (C) Scores for the two tools were plotted with values below the median in orange and above the median in purple. (D) Scores from ICE and TIDE tools were compared for a subset of six gRNAs compared to mosaicism percentages from Illumina sequencing of the same region. (E) From the PAGE, an empirical intensity ratio was obtained and compared to the *in vivo* efficiency scores. Spearman correlations results are shown in the scatter plots with the line of best fit included.

4
5
6
7
8
9
10
11
12
13
14

1 Accuracy of CRISPR on-target predictions by different methods

2 We next compared the accuracy of CRISPR on-target predictions computed by several published
3 algorithms, including CRISPRScan [26], CHOPCHOP [35, 36], E-CRISP [37], CRISP-GE [38],
4 CRISPR-RGEN [39], CCTop [40], as well as the design tool from Integrated DNA Technologies
5 (IDT, www.idtdna.com). Only five comparisons between tools exhibited significant correlations
6 in their predicted scores and these relationships were weak (Spearman $\rho < 0.5$; Figure 2). Only
7 CRISPRScan, which we used to design our gRNAs, exhibited significant, albeit weak,
8 correlation with *in vivo* experimentally determined values (Spearman $\rho = 0.32, p = 0.03$; Figure
9 2). Therefore, higher CRISPRScan scores predict higher *in vivo* efficiencies but with low
10 accuracy. Thus, despite the research community broadly adapting all methods, there is little
11 consensus in predicting activity of a particular gRNA among these tools. To assess if strain
12 variability may have impacted our analysis—since all prediction tools used the Tübingen-derived
13 reference genome (GRCz11) [4] whereas our study was performed in the NHGRI-1 strain (a
14 cross between wild-type strains AB and Tübingen [41])—we obtained re-calculated
15 CRISPRScan scores for our gRNAs using a modified zebrafish reference that included known
16 NHGRI-1 variants [41] (now available as an additional reference in the tool browser at
17 www.crisprscan.org). The CRISPRScan scores for the gRNAs using the new ‘NHGRIzed’
18 reference were highly concordant with the previous ones obtained with the Tübingen-derived
19 reference (Spearman $\rho = 0.88, p = 5.02 \times 10^{-17}$; Figure 2), with an average difference between
20 scores of 4.2 ± 4.6 (range 0–31) (Supplementary Table 2). Although we did observe large
21 differences in predicted efficiency scores (up to 31) for certain gRNAs between the two
22 reference backgrounds, overall the reference did not significantly impact our findings (Spearman
23 $\rho = 0.32$ (original) vs. 0.31 (NHGRIzed); Figure 2).

1



2

3 **Figure 2. Correlation of on-target efficiencies calculated using different methods.** Scores from *in silico*
4 prediction tools, an *in vitro* protocol [27], and cutting cleavages obtained *in vivo* using a deconvolution tool [33] for
5 50 gRNAs were compared using Spearman correlations. Each box includes the correlation result with the *p*-value in
6 parenthesis. The color of the boxes represent the correlation values , ranging between -1 (blue) and 1 (red).

7

8 Next, we evaluated the prediction power of the *in vitro* protocol CIRCLE-seq [27], an approach
9 designed to identify target sites of a given gRNA by subjecting naked genomic DNA to Cas9
10 enzyme/gRNA cleavage followed by Illumina sequencing. We tested individually the 50 gRNAs
11 described above using CIRCLE-seq [42] and computed a log enrichment score normalized by the
12 sequence library size, termed reads per million normalized (RPMN) (see Methods). We found
13 that *in vitro*-obtained enrichment scores were not correlated with *in vivo* efficiencies (Spearman
14 $\rho = -0.02, p = 0.91$; Figure 2) or with *in silico* predictions, indicating that the CIRCLE-seq assay
15 does not accurately predict on-target CRISPR cleavage activity, at least quantitatively. Previous

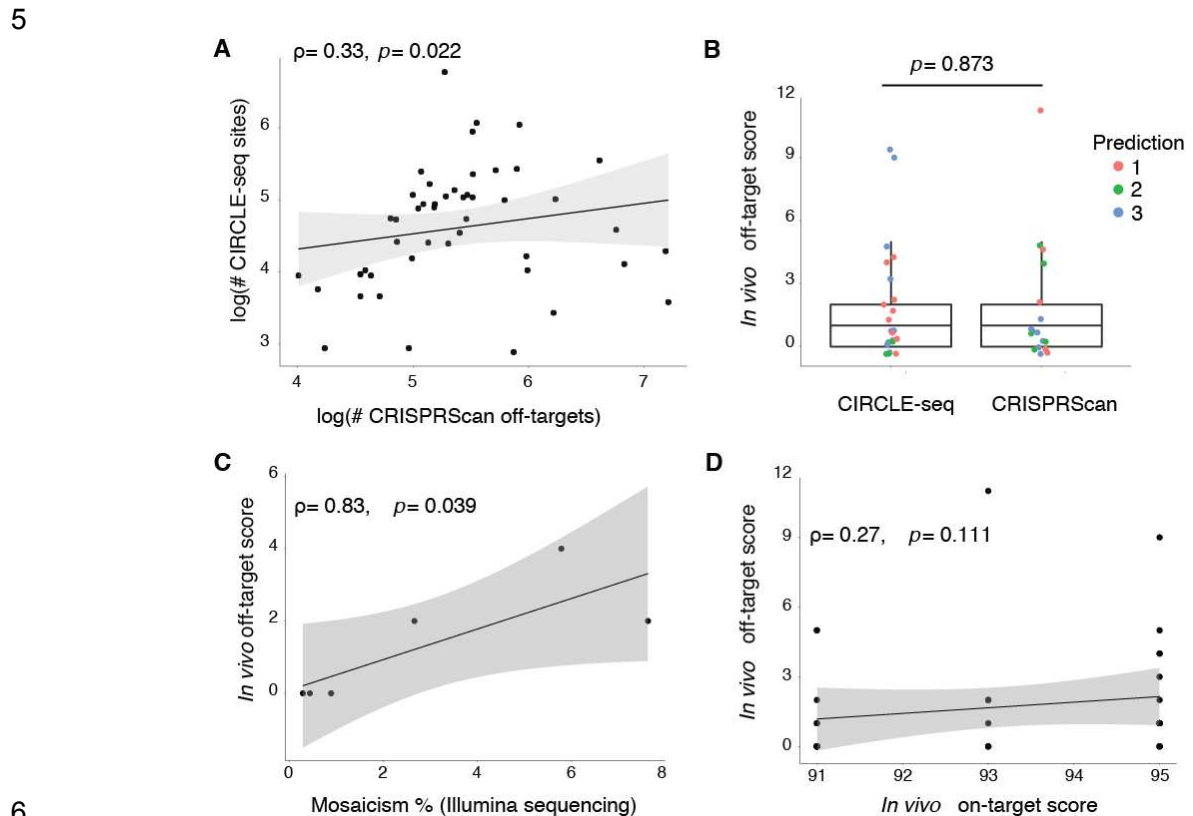
1 work from *in vivo* CRISPR studies of zebrafish suggests that increased GC-content predicts
2 increased activity of gRNAs [26]. Examining GC content of our tested gRNAs, ranging from
3 31.8 to 77.3%, we observed a positive correlation with CRISPRScan *in silico* scores (linear
4 model: beta= 68.18, $p= 0.003$, adjusted- $r^2= 0.16$) and CIRCLE-seq *in vitro* RPMN scores (linear
5 model: beta= 6.4, $p= 0.006$, adjusted- $r^2= 0.14$) (Supplementary Figures 1A and B); however, our
6 experimentally determined *in vivo* scores were not correlated with GC content (linear model:
7 beta=12.4, $p= 0.817$, adjusted- $r^2= -0.02$; Supplementary Figure 1C), suggesting that additional
8 variables should also be considered (e.g., depletion of A nucleotide bases, nucleosome
9 positioning or DNA accessibility [26, 43]).

10

11 **CRISPR off-target mutation prediction methods**

12 To avoid spurious phenotypes, off-target mutations should be minimized when choosing gRNAs
13 in CRISPR experiments. To characterize off-target mutations for our set of 50 gRNAs, we
14 queried predictions from *in silico* (CRISPRScan) and *in vitro* (CIRCLE-seq) methods.
15 CRISPRScan provides a list of predicted off-target sites (between 55 and 1,350, median 206.5;
16 Supplementary Table 3) for each gRNA within the zebrafish NHGRIzied reference genome
17 (GRCz11/danRer11) based on a cutting frequency determination (CFD) score that primarily
18 takes into account sequence similarity, location, and type of sequence mismatches [26, 44]. The
19 CIRCLE-seq empirical approach also produced variable numbers of sites (between 18 and 874,
20 median 113.5; Supplementary Table 3) per gRNA (defined as ‘CIRCLE-seq sites’) relative to the
21 control library digested solely with Cas9 enzyme. The number of off-target sites predicted by
22 CRISPRScan exhibited a significant, albeit weak, correlation with the number of CIRCLE-seq
23 sites per gRNA (Spearman $\rho=0.33$, $p= 0.022$, Figure 3A). Focusing on putatively impactful off-

1 target predictions, an average of $20 \pm 13\%$ CRISPRScan-predicted and $64 \pm 7\%$ CIRCLE-seq sites
2 per gRNA intersected at least one gene (Supplementary Table 3). The sites predicted *in silico* or
3 *in vitro* intersecting genes predominantly did not overlap with an average of 1.6 ± 1.8 (range 0-7)
4 genes per gRNA overlapping between the two approaches for the same gRNA.



7 **Figure 3. Assessment of off-target cleavage events using different prediction methods.** (A) The number of
8 predicted CRISPRScan off-target sites correlated with the number of identified CIRCLE-seq sites (Spearman
9 correlation). Log normalization was used to reduce the range in the number of sites. (B) *In vivo* editing scores from
10 the ICE tool for the top predicted off-target sites using CRISPRScan and CIRCLE-seq were not different. Scores
11 were compared using a Mann-Whitney U test. (C) Editing efficiencies at predicted off-target sites using *in vivo*
12 scores from Sanger sequencing and mosaicism % from Illumina sequencing were correlated (Spearman correlation).
13 (D) Editing scores obtained *in vivo* at off-target sites were not correlated with the on-target efficiency of the gRNA.
14 All scatter plots include the Spearman correlations results with the line of best fit.
15

16 To verify if predicted off-target sites were subjected to *in vivo* Cas9 cleavage, we performed
17 Sanger sequencing of sites within genes identified *in silico* (n= 17) and *in vitro* (n= 20) for eight
18 gRNAs with high *in vivo* efficiency scores (>90%), an average of six regions per gRNA (see
19 Supplementary Table 1 for description of sites). Using the ICE tool, we found mosaic mutations

1 at frequencies between 0 and 11%, with 23 out of the 37 sites evidencing indel frequencies
2 below 1% (Figure 3B), and no differences observed between off-target sites predicted by
3 CRISPRScan or CIRCLE-seq (Mann-Whitney $U= 175.5, p= 0.873$; Figure 3B). To validate the
4 accuracy of ICE at these low indel frequencies, we again performed Illumina sequencing of
5 predicted off-target sites for six of the eight evaluated gRNAs (see Supplementary Table 1 for
6 description) and found significant concordance in results (0.29–7.62% of mosaicism; Spearman
7 $\rho= 0.83, p= 0.039$; Figure 3C). The average difference in mosaicism between ICE and Illumina
8 was low (1.6 ± 2.0), with ICE tending to slightly underestimate indel frequencies, highlighting its
9 utility to quickly and economically assess predicted off-targets regions.

10

11 We also tested if sites predicted with higher likelihoods of off-target cutting events resulted in
12 higher mutation rates by comparing the indel frequencies among the different levels of prediction
13 (top 1, 2, or 3 prediction scores by CRISPRScan or CIRCLE-seq). No differences were found
14 between prediction groups (Kruskal-Wallis: $H_{(2)}= 2.26, p= 0.320$; Figure 3B), suggesting that the
15 information used by the tools to assign probabilities of off-target activity (e.g., CFD scores in
16 CRISPRScan or normalized read counts in CIRCLE-seq) do not necessarily predict the
17 efficiency of cutting at off-target sites. Thus, off-target cutting mutations at the assessed sites
18 exhibited low frequencies with no clear method performing best. Moreover, none of the on-target
19 scores previously obtained (*in silico*, *in vitro*, or *in vivo*) correlated with the number of *predicted*
20 off-target sites per gRNA (using either CRISPRScan or CIRCLE-seq), nor the frequency of
21 indels at validated off-target sites (Spearman $\rho= 0.27, p= 0.111$, Figure 3D), suggesting that
22 higher on-target efficiencies do not necessarily translate into increased frequencies of spurious
23 off-target mutations.

1 **Evaluating CRISPR Cas9-injection controls**

2 A commonly used ‘mock’ injection control for phenotypic screens of CRISPR-generated G₀
3 mosaic lines are embryos injected with buffer and Cas9 in the absence of a gRNA. We sought to
4 determine if such control treatments could significantly impact the genome or transcriptome of
5 our zebrafish larvae. To characterize its impact on genes, we performed RNA-seq of wild-type
6 NHGRI-1 embryos injected with either Cas9 enzyme or Cas9 mRNA (three pools of five
7 injected larvae each), uninjected batch siblings (two pools of five larvae), and uninjected siblings
8 from another batch (three pools of five larvae) as controls.

9

10 *Potential genomic mutations in controls*

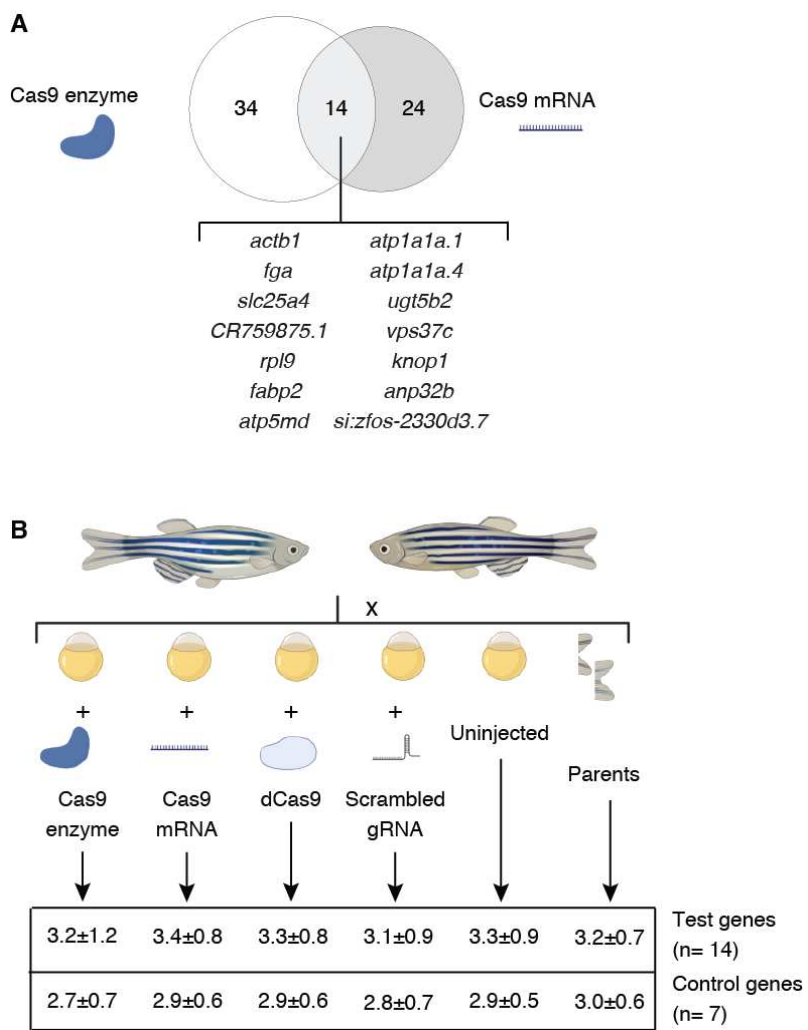
11 Recently, Sundaresan and colleagues [45] found that Cas9 in the presence of Mn⁺² ions can
12 result in double-strand cleavage of genomic DNA in the absence of a gRNA. Although their
13 study did not show this same off-target cleavage activity in the presence of Mg⁺², we
14 hypothesized that aberrant genomic mutations could be incurred by Cas9 due to the presence of
15 MgCl₂ in our injection buffer since Mg⁺² has been shown to compete with Mn⁺² in activating
16 common enzymes [46]. Using our RNA-seq data, we used an optimized pipeline [47] to identify
17 somatic mosaic mutations with uninjected wild-type controls as a reference for common
18 polymorphisms. Focusing only on high-confidence variants (minimum sequence read depth of
19 20), we filtered already reported variants in the NHGRI-1 zebrafish line [41], and used the
20 Variant Effect Predictor tool from ENSEMBL to obtain a list of frameshift mutations in protein-
21 coding genes present in our Cas9-injected larvae. A total of 48 and 38 genes were identified with
22 frameshifting variants in larvae injected with Cas9-enzyme and Cas9-mRNA, respectively, with
23 14 of these genes shared across both injection types (Figure 4A, Supplementary Table 4). On

1 average, each pool of larvae injected with Cas9 enzyme or mRNA carried frameshift variants in
2 18.7±3.1 genes. All identified frameshift variants evidenced low allelic frequencies (Cas9-
3 enzyme: average 0.043, range 0.0036-0.142; Cas9-mRNA: average 0.059, range 0.002-0.316)
4 and high read depth (Cas9-enzyme: average 386.5, range 22-2076; Cas9-mRNA: average 343.8,
5 range 20-3453) (Supplementary Table 4). Additionally, frameshift variants were positioned
6 closer to a potential Cas9 PAM site (NGG) than by random chance (4 bp median observed
7 distance to closest PAM site; empirical $p= 0.0016$ using the whole-genome and $p= 0.006$ using
8 protein-coding regions only, from 10,000 permutations). Therefore, we decided to evaluate if
9 indels would consistently arise in these genes in an additional set of microinjections.

10

11 We performed a new set of microinjections in NHGRI-1 larvae using these same controls (Cas9
12 enzyme and Cas9 mRNA) and two additional ones commonly used in CRISPR experiments
13 (catalytically dead Cas9 (dCas9) enzyme and a scrambled gRNA coupled with Cas9 enzyme,
14 sequence published in [19]) and evaluated the presence of mutations in 21 genes, including 14
15 genes with identified frameshift mutations in our RNA-seq data and seven controls with no
16 mutations observed (Figure 4B, see Supplementary Table 1 and Supplementary Table 5 for the
17 description of all sites). Briefly, genomic DNA was harvested from (1) three pools of five larvae
18 from each group injected at the one-cell stage (Cas9 enzyme, Cas9 mRNA, dCas9, scrambled
19 gRNA); (2) three pools of five uninjected batch siblings larvae; and (3) finclips of the crossing
20 parents as controls. Subsequently, ~200 bp regions surrounding the closest Cas9 PAM site to the
21 previously RNA-seq-identified variants were Illumina sequenced and the alleles extracted using
22 *CrispRVariants* [34]. We did not observe evidence of inflation of indels in any of the injected
23 groups relative to the uninjected batch siblings or the parental fish, with an overall average

1 mosaicism of $3.1 \pm 0.8\%$ per site (below the expected 10% allele ratio for a heterozygous variant
2 in a single individual from a pool of five; Figure 4B, Supplementary Table 5). Our NHGRI-1
3 zebrafish carried common single nucleotide variants in the targeted regions, particularly in gene
4 (Supplementary Figure 2). Interestingly, we did observe a subtly higher mosaicism in the genes
5 (*si:ch1073-110a20* where two variants were present in close to 50% and 20% of the reads
6 previously detected with variants in our RNA-seq data relative to the regions used as controls



7
8 **Figure 4. Evaluation of spurious genomic mutations in CRISPR-injection controls. (A)** The abundance of
9 protein-coding genes carrying frameshift variants for each Cas9-injected treatment are depicted in a Venn diagram,
10 with mutated genes identified in both treatments listed. **(B)** Genomic DNA from zebrafish larvae injected with Cas9
11 enzyme, Cas9 mRNA, catalytically dead Cas9 (dCas9), a scrambled gRNA, uninjected batch siblings, and a fin clip
12 from their parents was used to perform targeted Illumina sequencing of 21 genes to quantify indel mosaicism with
13 average \pm standard deviation values listed in the table (see Supplementary Table 1 and Supplementary Table 7 for
14 the description of the genes).

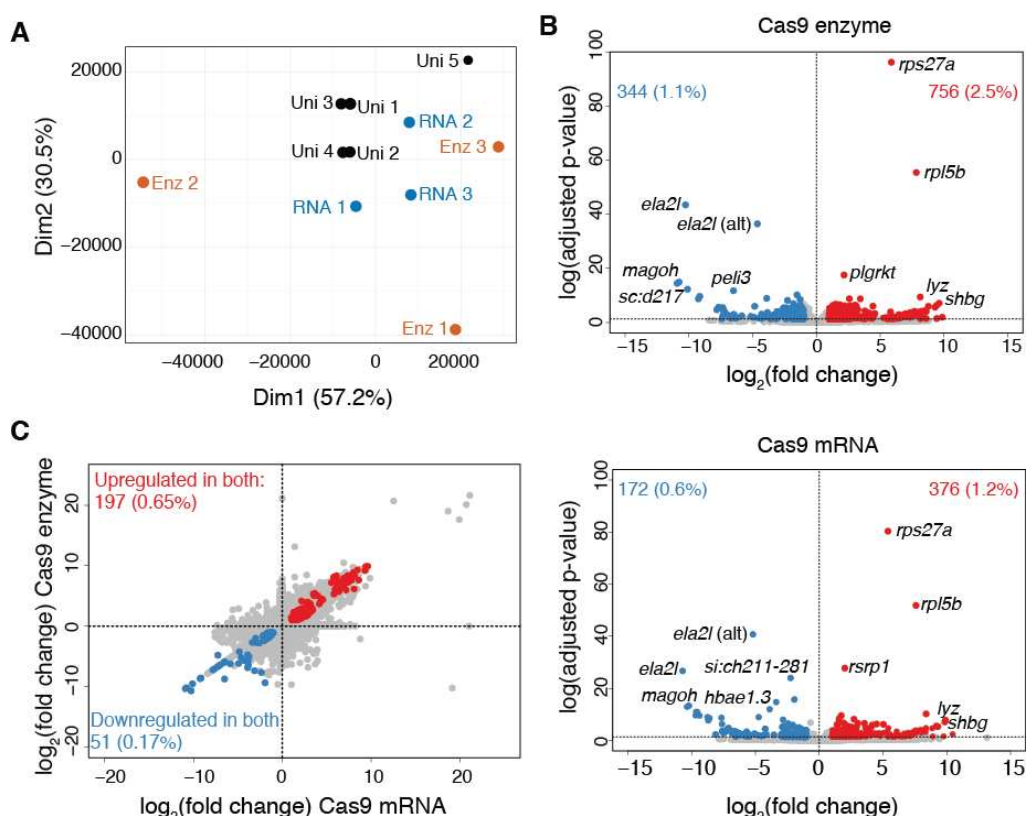
1 (Mann-Whitney $U=2251.5$, $p=0.00074$, median mosaicism in tested genes 3.4%, median
2 mosaicism in control genes 2.88%; Figure 4B, Supplementary Table 5). Thus, it is possible that
3 the genes we identified with variants in our RNA-seq data may be naturally prone to carry
4 variants. In summary, these results suggest that currently used CRISPR controls do not suffer
5 systematic DNA cleavages in the absence of a gRNA.

6

7 *Differential gene expression in controls*

8 We also characterized the impact of injecting Cas9 enzyme or mRNA on the transcriptomes of
9 our zebrafish larvae. Comparisons of transcripts abundances show significant variance across
10 biological replicates when quantifying in both Cas9 treatments, particularly evident in samples
11 injected with the Cas9 enzyme, versus wild-type uninjected larvae (Figure 5A). This suggests
12 that considerable stochasticity may exist regarding the effects of Cas9 injections in these
13 controls. Examining the genes impacted, we identified hundreds of differentially-expressed (DE)
14 genes in our Cas9-injected versus uninjected controls, with a greater number of upregulated
15 genes than downregulated genes (Figure 5B, Supplementary Table 6). Specifically, Cas9-enzyme
16 injections resulted in a total of 1,100 DE genes (3.6% of the genes assayed), with 756 genes
17 (68.7%) upregulated (fold change > 1) and 344 (31.3%) downregulated (fold change < -1). Cas9-
18 mRNA injected larvae exhibited 548 DE genes (1.8% of the genes assayed), 376 (68.6%) of
19 these upregulated and 172 (31.4%) downregulated (Figure 5B). We observed 248 (197
20 upregulated and 51 downregulated) common DE genes between the two treatments (Figure 5C),
21 which could be part of a common response to the microinjection process. Network analyses
22 identified commonalities in the shared DE genes enriched in key regulators of different KEGG
23 pathways, including spliceosome and ribosome (including genes *eif4g2b*, *eif4g1a*, *hnrnpd*,

1 *magoh*, *hnrnpa0a*), hedgehog signaling (*shha*), glutathione metabolism (*gsto2*, *gsr*), GnRH
2 signaling (*dusp6*), aminoacyl-tRNA biosynthesis (*yars*), cell cycle (*kif2c*), glycolysis (*aldoca*),
3 and cellular senescence (*ppp3cca*) (Supplementary Figure 3). Furthermore, while we observed
4 no enrichment in gene ontology terms for downregulated genes, common upregulated genes
5 from both treatments were related to response to wounding (GO:0009611, adjusted *p*-value=
6 0.009) and cytoskeleton organization (GO:0045104, adjusted *p*-value=0.009) (Supplementary
7 Table 7), revealing molecular consequences of the microinjection process that were still
8 detectable five days later.



9
10 **Figure 4. Evaluation of spurious genomic mutations in CRISPR-injection controls.** (A) The abundance of
11 protein-coding genes carrying frameshift variants for each Cas9-injected treatment are depicted in a Venn diagram,
12 with mutated genes identified in both treatments listed. (B) Genomic DNA from zebrafish larvae injected with Cas9
13 enzyme, Cas9 mRNA, catalytically dead Cas9 (dCas9), a scrambled gRNA, uninjected batch siblings, and a fin clip
14 from their parents was used to perform targeted Illumina sequencing of 21 genes to quantify indel mosaicism with
15 average \pm standard deviation values listed in the table (see Supplementary Table 1 and Supplementary Table 7 for
16 the description of the genes).
17

1 **DISCUSSION**

2 Our study presents a comprehensive evaluation of empirical and predictive tools currently used
3 for CRISPR editing in zebrafish. Cleavage scores obtained by an *in vivo* assessment of 50
4 gRNAs via Sanger sequencing and deconvolution tools (ICE and TIDE) were highly concordant,
5 as previously reported [33], but only ICE scores were correlated in cases of higher (>50%)
6 mosaicism percentages with Illumina sequencing, the commonly used gold standard. ICE scores
7 tended to underestimate the presence of non-edited alleles by ~20% for gRNAs with high
8 efficiencies (>50% cutting efficiency), contrary to previous comparisons of TIDE and Illumina
9 sequencing in cell lines, where TIDE showed a ~10–20% overestimation of non-edited alleles
10 [48]. For sites with lower indel frequencies, as we observed for predicted off-target mutations,
11 ICE scores were more concordant with Illumina results (~1–2% difference, again mostly
12 underestimates). Therefore, we suggest that Sanger sequencing deconvolution tools are valuable
13 for establishing relative gRNAs efficiencies but do not necessarily accurately predict absolute
14 cleavage efficiencies in zebrafish *in vivo*, except at sites with low indel frequencies. In addition,
15 we formalized an empirical ‘intensity ratio’ score from the commonly-used PAGE approach to
16 assay CRISPR indels and verified its utility in approximating cleavage efficiencies, making it a
17 more affordable and rapid approach to assay editing efficiencies versus sequencing.

18

19 On-target efficiency prediction tools showed large differences using the same set of gRNAs
20 sequences, highlighting the importance of understanding features accounted for by each tool. A
21 recent review [25] provides a comprehensive overview of different design tools available and the
22 source of experimental data used to train each one. Compared with our *in vivo* efficiency scores
23 from zebrafish embryos, CRISPRScan [26] was the only tool that could predict on-target

1 efficiency in our set of gRNAs, while no other method provided scores that were correlated with
2 cleavage activities observed *in vivo*. Notably, although significant genetic variation exists
3 between zebrafish strains [49, 50], we found no global change in prediction accuracy when using
4 the current reference genome derived from the Tübingen strain [4] versus an NHGRIzed
5 reference [41] used in our study and comparing with our *in vivo* scores. Overall, our results
6 emphasize the importance of utilizing a tool that has been trained using experimental data
7 specifically from zebrafish.

8

9 An *in silico* (CRISPRScan) and *in vitro* (CIRCLE-seq) method predicted ~20% and 65%
10 potential off-target regions impacting genes, respectively. Notably, we did not evaluate if other
11 predicted sites included *cis*-regulatory elements that could also potentially alter gene expression.
12 Future assessments should include tests targeting a diversity of loci for a more thorough
13 understanding of the potential off-target indels caused by unwanted CRISPR cleavage sites. We
14 observed low off-target mutation frequencies (most <1%), similar to those previously reported
15 from using single [11, 12] or multiple gRNAs [18], although did observe off-target indel
16 frequencies as high as 11% for certain gRNAs. Notably, neither predictive method (CRISPRScan
17 or CIRCLE-seq) nor their likelihood score (using CFD or normalized read count) could
18 accurately predict indel frequencies at off-target sites. Typically, such low mutation frequencies
19 should not be of high impact when generating stable knockout zebrafish lines as these could be
20 easily outcrossed. However, such mutations could have significant impacts on phenotypic
21 outcomes when injected G₀ mosaic populations are analyzed directly.

22

1 The adequate selection of controls is a fundamental process in evaluating gene function using G₀
2 knockout crispant zebrafish, as these larvae serve as baselines from which inferences will be
3 made from. Currently, no consensus exists for preferred controls used in high-throughput
4 CRISPR workflows of zebrafish larvae, which can include targeting a known gene as a positive
5 control (e.g., *tyr*) [14], uninjected larvae [17, 18], sham injections with a Cas9:tracrRNA
6 complex [15], and injections of a scrambled gRNA [16, 19], among others. Our RNA-seq assay
7 identified several genes carrying frameshift mutations using uninjected clutch siblings as
8 reference. A follow-up analysis of a second set of injections showed existence of mosaic variants
9 in all injected controls (e.g., Cas9 mRNA, enzyme, and scrambled gRNA), in addition to
10 uninjected siblings and crossed parents at low allelic frequencies (~3%). Nevertheless, even
11 though we were limited to our targeted regions, we did observe a higher mosaicism in genes
12 identified as carrying frameshift mutations from our RNA-seq assay compared to control genes,
13 suggesting that these genes could be naturally prone to exhibit mutations in the NHGRI-1
14 zebrafish line. We also observed high variability in gene expression in larvae solely injected with
15 Cas9 enzyme or mRNA, with several of these DE genes involved in response to wounding
16 processes. Notably, these DE genes were retrieved from 5 dpf larvae suggesting that damage
17 incurred during the microinjection process has a lasting effect.

18

19 CONCLUSIONS

20 Overall, we performed a simultaneous assessment of gRNA activities predicted by several
21 commonly used *in silico* and *in vitro* methods with those determined experimentally *in vivo* in
22 injected zebrafish embryos. These results provide valuable information that can be incorporated
23 into the design and execution of CRISPR/Cas9 assays in zebrafish using available workflows [8,

1 13, 14, 17, 18]. Our aim was to provide information to aid in the decision-making process for
2 future projects using affordable and reliable gene-editing tools in zebrafish. As higher-
3 throughput methods continue to be developed for assaying multiple genes simultaneously, it will
4 be important to use optimal tools for predicting and assessing on- and off-target activity in
5 zebrafish larvae for accurate interpretation of phenotypic outcomes.

6

7 **METHODS**

8 **Zebrafish husbandry**

9 NHGRI-1 wild type zebrafish lines [41] were maintained through standard protocols [51] and
10 naturally spawned to obtain embryos. All animal use was approved by the Institutional Animal
11 Care and Use Committee from the Office of Animal Welfare Assurance, University of
12 California, Davis.

13

14 **Design and *in silico* predictions for gRNAs**

15 50 gRNAs targeting exons of 14 genes were designed using CRISPRScan [26] (scores ranging
16 between 24 and 83 with a mean value of 57.60) with zebrafish genome version
17 GRCz11/danRer11 as the reference (see description of gRNAs in Supplementary Tables 1 and
18 2). All targeted genes were protein coding. For each designed gRNA, we obtained the efficiency
19 scores predicted by CRISPRScan [26], CHOPCHOP [35], E-CRISP [37], CRISPR-GE [38],
20 CRISPR-RGEN [39], CCTop [40], and the IDT design tool (www.idtdna.com). From
21 CRISPRScan, we also gathered the top 30 predicted off-target sites for each gRNA defined by
22 the CFD score [26]. Additionally, we utilized *bedtools* [52] to determine the GC percentage for
23 each gRNA. To incorporate NHGRI-1 variants into the zebrafish reference, we used the

1 FastaAlternateReferenceMaker function from *GATK* [53] with the reported high-confidence
2 variants for the NHGRI-1 zebrafish strain [41].

3

4 **Microinjections to generate CRISPR G₀ mosaic mutants**

5 All gRNAs were individually injected into NHGRI-1 embryos to estimate the frequency of
6 indels. gRNAs were prepared following the manufacturer's protocol (Integrated DNA
7 Technologies). Briefly, 2.5 μ l of 100 μ M crRNA, 2.5 μ l of 100 μ M tracrRNA, and 5 μ l of
8 Nuclease-free Duplex Buffer using an annealing program consisting of 5 min at 95°C, a ramp
9 from 95°C to 50°C with a -0.1°C/s change, 10 minutes (min) at 50°C, and a ramp from 50°C to
10 4°C with a -1°C/s change. Ribonucleoprotein injection mix was prepared with 1.30 μ l of Cas9
11 enzyme (20 μ M, New England BioLabs), 1.60 μ l of prepared gRNAs, 2.5 μ l of 4x Injection
12 Buffer (containing 0.2% phenol red, 800 mM KCl, 4 mM MgCl₂, 4 mM TCEP, 120 mM HEPES,
13 pH 7.0), and 4.6 μ l of Nuclease-free water. Microinjections directly into the yolk of NHGRI-1
14 embryos at the one-cell stage were performed as described previously [54], using needles from a
15 micropipette puller (Model P-97, Sutter Instruments) and an air injector (Pneumatic MPPI-2
16 Pressure Injector). Embryos were collected and ~1 nl of ribonucleoprotein mix was injected per
17 embryo, after previous calibration with a microruler. Twenty injected embryos per Petri dish
18 were grown up to 5 dpf at 28°C.

19

20 **Sanger and Illumina amplicon sequencing**

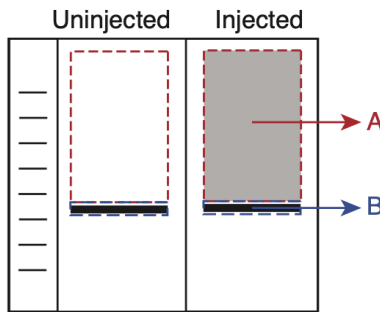
21 DNA extractions were performed on 20 pooled embryos by adding 100 μ l of 50 mM NaOH,
22 incubation at 95°C for 20 min, ramp from 95°C to 4°C at a 0.7°C/s decrease, followed by an
23 addition of 10 μ l of 1 M Tris-HCl and a 15 min spin at 4680 rpm. We amplified a ~500 bp region

1 surrounding the targeted site of each gRNA (see Supplementary Table 1 for description of
2 primers). PCR amplifications were performed using 12.5 μ l of 2X DreamTaq Green PCR Master
3 Mix (Thermo Fisher), 9.5 μ l of Nuclease-Free water, 1 μ l of 10 μ M primers, and 1 μ l extracted
4 DNA. Thermocycler program included 3 min at 95°C, followed by 35 cycles of 15 s at 95°C, 30
5 s at 60°C, and 20 s at 72°C, and a final 5 min incubation at 72°C. Reactions were purified using
6 Ampure XP magnetic beads (Beckman Coulter) and Sanger sequenced (Genewiz, San Diego,
7 CA). Raw trace files were used in the TIDE [32] and ICE [33] tools to predict the percentage of
8 indels, which we used as our *in vivo* editing score for each gRNA. To compare accuracy between
9 these tools, we PCR amplified ~200 bp around the targeted regions from the same extracted
10 DNA for six gRNAs and performed Illumina sequencing (Genewiz, San Diego, CA) to obtain
11 percent mosaicism of mutants by mapping paired-end fastq reads to the zebrafish reference
12 genome (GRCz11/danRer11) using *bwa* [55] and the R package *CrispRVariants* [34]. For both
13 Sanger and Illumina sequencing, we used uninjected batch-sibling embryos as a control
14 reference.

15

16 PAGE and intensity-ratio estimation

17 An empirical cleavage analysis from each gRNA was performed using PAGE. Briefly, we
18 amplified a ~200 bp region in DNA around the targeted site from gRNA-injected and uninjected
19 embryos, as described above. Reactions were run on 7.5% polyacrylamide gels for 75 min at 110
20 V and revealed using GelRed (VWR International). Gel images were processed in the software
21 Fiji [56]. For each sample, we defined areas **A** and **B** as follows:



1
2 For each gRNA, the mean-intensity value was obtained for the A and B areas in both the injected
3 and uninjected samples. The A and B areas were exactly the same size between samples. The
4 intensity ratio was calculated as: [injected B / injected A] / [uninjected B / uninjected A]. Log-
5 normalized intensity ratios followed a normal distribution (Shapiro-Wilk test: $W=0.96$, $p=$
6 0.167) with an average value of 1.21 ± 0.70 .

7

8 CIRCLE-seq

9 CIRCLE-seq libraries were prepared for each gRNA (IDT) using genomic DNA extracted from
10 NHGRI-1 (DNA Blood & Tissue kit, Qiagen) following the described protocol [42]. Libraries
11 were sequenced using one HiSeq XTen lane (Novogene, Sacramento, CA), providing an average
12 of 7.3 million reads (range: 4.0 - 13.3 million reads) and $>Q30$ for 92% of reads per gRNA
13 library. Raw reads were processed using the bioinformatic pipeline described [42] to identify
14 regions with cutting events relative to a control sample (treated with Cas9 enzyme and no
15 gRNA). To obtain an on-target efficiency estimation from *in vitro* digestions, we calculated the
16 reads per million normalized (RPMN). For this purpose, we used *samtools* [55] to extract read
17 coverage from aligned bam files. For each gRNA, coverage was obtained for the third and fourth
18 base upstream of the PAM site as it is the region expected to be cut by Cas9 [57]. RPMN for
19 each gRNA was calculated as the sum of coverage at these two sites divided by the total mapped

1 reads per sample and multiplied by one million to scale the values. RPMN scores ranged from
2 4.42 to 881 (median 99.3) so we decided to use a log normalization to reduce this range.

3

4 **RNA-seq**

5 We performed RNA-seq of Cas9 injected NHGRI-1 larvae to identify potential gRNA-
6 independent cleavage sites. One-cell stage NHGRI-1 embryos were injected with either Cas9
7 enzyme or Cas9 mRNA. Injection mix for Cas9 enzyme included Cas9 enzyme (20 μ M, New
8 England BioLabs), 2.5 μ l of 4x Injection Buffer (0.2% phenol red, 800 mM KCl, 4 mM MgCl₂, 4
9 mM TCEP, 120 mM HEPES, pH 7.0), and Nuclease-free water. Cas9 mRNA was obtained from
10 plasmid pT3TS-nCas9n (Addgene, plasmid #46757) [5], using the MEGAshotscript T3
11 transcription kit (Thermo Fisher) following manufacturer's guidelines of 3.5 h 56°C incubation
12 with T3. mRNA was purified with the MEGAclear transcription clean-up kit (Thermo Fisher)
13 and concentration of mRNA obtained using a NanoDrop (Thermo Fisher). The injection mix of
14 Cas9 mRNA contained 100 ng/ μ l of mRNA, 4x Injection Buffer (0.2% phenol red, 800 mM
15 KCl, 4 mM MgCl₂, 4 mM TCEP, 120 mM HEPES, pH 7.0), and Nuclease-free water.
16 Additionally, uninjected batch-siblings and uninjected siblings from an additional batch were
17 used as controls. All embryos were grown at 28°C in a density of <50 embryos per dish. At 5
18 dpf, three pools of five larvae were collected for each group (Cas9 enzyme, Cas9 mRNA, and
19 uninjected) for RNA extraction using the RNeasy kit (Qiagen) with genomic DNA eliminator
20 columns for DNA removal. Whole RNA samples were subjected to RNA-seq using the poly-A
21 selection method (Genewiz, San Diego, CA).

22

23 **Variant identification from RNA-seq data**

1 We followed a previously described pipeline to identify somatic variants from RNA-seq data
2 [47]. Briefly, we mapped reads with *STAR* [58] using the 2-pass mode and a genomic reference
3 created with GRCz11/danRer11 assembly and gtf files (release version 100). Variant calling was
4 performed with MuTect2 as part of *GATK* [53] using the tumor versus normal mode. ‘Normal’
5 was defined by the two uninjected samples to identify all somatic mutations in our Cas9 injected
6 embryos. Variants were annotated using the Variant Effect Predictor tool [59]. High confidence
7 variants (minimum sequencing depth of 20) previously reported for the NHGRI-1 line [41] were
8 removed. Only frameshift loss-of-function variants with a minimum read depth of 20 in
9 canonical protein-coding genes were considered. We extracted the median distance between the
10 identified variants and the nearest Cas9 PAM site (NGG sequence) using the coordinates in the
11 CRISPRScan UCSC track. This median observed distance was compared to the result of median
12 distances of 10,000 permutations of random sampling across the genome and their nearest PAM
13 site. One-tailed empirical *p* values from this comparison were calculated as $(M+N)/(N+1)$, where
14 *M* is the number of iterations with a median distance below the observed value and *N* is the total
15 number of iterations. We orthogonally investigated the presence of variants in 23 genes via
16 Illumina sequencing of a ~200 bp region surrounding the identified variant location and the R
17 package *CrispRVariants* [34] (Supplementary Table 1 for primers description). For this purpose,
18 we extracted DNA from 3 pools of 5 embryos injected with Cas9 enzyme, Cas9 mRNA, dCas9
19 (Alt-R S. p. dCas9 protein V3 from IDT), a scrambled gRNA (see Supplementary Table 1 for
20 sequence description), or uninjected. In addition, we extracted DNA from a finclip of the
21 crossing parents of the embryos used for the injections (both female and male). In all of these
22 groups, we quantified the percentage of mutations as all alleles different from the reference.
23

1 **Differential gene expression analysis from RNA-seq data**

2 Raw reads were processed using the *elvers* (<https://github.com/dib-lab/elvers>; version 0.1,
3 release DOI: 10.5281/zenodo.3345045) bioinformatic pipeline that utilizes *fastqc* [60],
4 *trimmomatic* [61], and *salmon* [62] to obtain the transcripts per kilobase million (TPM) for each
5 gene. *DESeq2* [63] was used to extract differentially-expressed genes in the Cas9 enzyme or
6 Cas9 mRNA injected samples relative to the uninjected larvae. R package *clusterProfiler* [64]
7 was used to perform enrichment tests of differentially-expressed genes in biological pathways.
8 Network analyses of the common differential expressed genes was performed using the
9 NetworkAnalyst online tool (www.networkanalyst.ca) [65, 66].

10

11 **Statistical analyses**

12 All analyses were performed in R version 4.0.2 [67]. Normality of variables was checked using
13 the Shapiro-Wilk test and parametric or nonparametric comparisons made accordingly.
14 Spearman correlation tests (denoted as ρ) and linear regression models were used to determine
15 the relationship between variables. All analyses compared across different experimental batches
16 included *batch* as a factor in the model to prevent biases caused by inter-batch differences.
17 Averages include the standard deviation unless otherwise specified. Alpha to determine
18 significance across the different tests was set at 0.05 unless otherwise specified. Additional R
19 packages used for making figures included *eulerr* [68].

20

21 **Abbreviations**

1 CFD: cutting frequency determination; CRISPR: clustered regularly interspaced short
2 palindromic repeats; gRNA: guide RNA; indels: insertions or deletions; PAGE: polyacrylamide
3 gel electrophoresis; RPMN: reads per million normalized.

4

5 **DECLARATIONS**

6 **Ethics approval and consent to participate**

7 Animal use was properly approved by the Institutional Animal Care and Use Committee from
8 the Office of Animal Welfare Assurance, University of California, Davis.

9

10 **Consent for publication**

11 Not applicable.

12

13 **Availability of data and materials**

14 Original fastq files from the CIRCLE-seq and RNA-seq assays are deposited in the European
15 Nucleotide Archive repository under project PRJEB39643.

16

17 **Competing interests**

18 The authors declare that they have no competing interests.

19

20 **Funding**

21 This work was supported, in part, by the U.S. National Institutes of Health (NIH) grants from the
22 National Institute of Neurological Disorder and Stroke (R00NS083627 to M.Y.D.), the Office of
23 the Director and National Institute of Mental Health (DP2 OD025824 to M.Y.D.), UC Davis

1 MIND Institute Intellectual and Developmental Disabilities Research Center pilot grant (U54
2 HD079125 to M.Y.D.), and a UC Davis Graduate Research Award (J.M.U-S.). The content is
3 solely the responsibility of the authors and does not necessarily represent the official views of the
4 National Institutes of Health. M.Y.D. is also supported by a Sloan Research Fellowship (FG-
5 2016-6814). The funding sources did not play a role in the research or publication process.

6

7 **Authors' contributions**

8 JMUS: conceptualization, data collection, analysis, writing of the article. AS, GK, KW, and CI:
9 data collection. MYD: conceptualization, funding acquisition, analysis, writing of the article. All
10 authors have read and approved the manuscript.

11

12 **Acknowledgements**

13 We thank our team of UC Davis undergraduate students that maintain husbandry to keep our
14 zebrafish healthy and happy. Thank you to Dr. Li-En Jao for kindly providing the Cas9 mRNA
15 plasmid and comments on the manuscript, and Daniela C. Soto for bioinformatic support. We are
16 grateful to Dr. Charles Vejnar and Dr. Antonio Giraldez for the incorporation of our NHGRIzied
17 zebrafish reference to the CRISPRScan online tool.

18

19 **REFERENCES**

20 1. Meyers JR. Zebrafish: Development of a Vertebrate Model Organism: Zebrafish :
21 Development of a Vertebrate Model Organism. Current Protocols Essential Laboratory
22 Techniques. 2018;16:e19.

23 2. Holtzman NG, Iovine MK, Liang JO, Morris J. Learning to Fish with Genetics: A Primer on
24 the Vertebrate Model Danio rerio. Genetics. 2016;203:1069–89.

25 3. Liu J, Zhou Y, Qi X, Chen J, Chen W, Qiu G, et al. CRISPR/Cas9 in zebrafish: an efficient

1 combination for human genetic diseases modeling. *Hum Genet*. 2017;136:1–12.

2 4. Howe K, Clark MD, Torroja CF, Torrance J, Berthelot C, Muffato M, et al. The zebrafish
3 reference genome sequence and its relationship to the human genome. *Nature*. 2013;496:498–
4 503.

5 5. Jao L-E, Wente SR, Chen W. Efficient multiplex biallelic zebrafish genome editing using a
6 CRISPR nuclease system. *Proc Natl Acad Sci U S A*. 2013;110:13904–9.

7 6. Hwang WY, Fu Y, Reyon D, Maeder ML, Tsai SQ, Sander JD, et al. Efficient genome editing
8 in zebrafish using a CRISPR-Cas system. *Nat Biotechnol*. 2013;31:227–9.

9 7. Irion U, Krauss J, Nüsslein-Volhard C. Precise and efficient genome editing in zebrafish using
10 the CRISPR/Cas9 system. *Development*. 2014;141:4827–30.

11 8. Varshney GK, Pei W, LaFave MC, Idol J, Xu L, Gallardo V, et al. High-throughput gene
12 targeting and phenotyping in zebrafish using CRISPR/Cas9. *Genome Res*. 2015;25:1030–42.

13 9. Vejnar CE, Moreno-Mateos MA, Cifuentes D, Bazzini AA, Giraldez AJ. Optimized CRISPR-
14 Cas9 System for Genome Editing in Zebrafish. *Cold Spring Harb Protoc*. 2016;2016.
15 doi:10.1101/pdb.prot086850.

16 10. Chang N, Sun C, Gao L, Zhu D, Xu X, Zhu X, et al. Genome editing with RNA-guided Cas9
17 nuclease in zebrafish embryos. *Cell Res*. 2013;23:465–72.

18 11. Hruscha A, Krawitz P, Rechenberg A, Heinrich V, Hecht J, Haass C, et al. Efficient
19 CRISPR/Cas9 genome editing with low off-target effects in zebrafish. *Development*.
20 2013;140:4982–7.

21 12. Burger A, Lindsay H, Felker A, Hess C, Anders C, Chiavacci E, et al. Maximizing
22 mutagenesis with solubilized CRISPR-Cas9 ribonucleoprotein complexes. *Development*.
23 2016;143:2025–37.

24 13. Gagnon JA, Valen E, Thyme SB, Huang P, Akhmetova L, Pauli A, et al. Efficient
25 mutagenesis by Cas9 protein-mediated oligonucleotide insertion and large-scale assessment of
26 single-guide RNAs. *PLoS One*. 2014;9:e98186.

27 14. Varshney GK, Carrington B, Pei W, Bishop K, Chen Z, Fan C, et al. A high-throughput
28 functional genomics workflow based on CRISPR/Cas9-mediated targeted mutagenesis in
29 zebrafish. *Nat Protoc*. 2016;11:2357–75.

30 15. Watson CJ, Monstad-Rios AT, Bhimani RM, Gistelinck C, Willaert A, Coucke P, et al.
31 Phenomics-Based Quantification of CRISPR-Induced Mosaicism in Zebrafish. *Cell Syst*.
32 2020;10:275–86.e5.

33 16. Wu RS, Lam II, Clay H, Duong DN, Deo RC, Coughlin SR. A Rapid Method for Directed
34 Gene Knockout for Screening in G0 Zebrafish. *Dev Cell*. 2018;46:112–25.e4.

1 17. Hoshijima K, Juryneec MJ, Klatt Shaw D, Jacobi AM, Behlke MA, Grunwald DJ. Highly
2 Efficient CRISPR-Cas9-Based Methods for Generating Deletion Mutations and F0 Embryos that
3 Lack Gene Function in Zebrafish. *Dev Cell*. 2019;51:645–57.e4.

4 18. Shah AN, Davey CF, Whitebirch AC, Miller AC, Moens CB. Rapid Reverse Genetic
5 Screening Using CRISPR in Zebrafish. *Nature Methods*. 2015;12:152–3.

6 19. Kroll F, Powell GT, Ghosh M, Gestri G, Antinucci P, Hearn TJ, et al. A simple and effective
7 F0 knockout method for rapid screening of behaviour and other complex phenotypes. *Elife*.
8 2021;10. doi:10.7554/eLife.59683.

9 20. Thyme SB, Pieper LM, Li EH, Pandey S, Wang Y, Morris NS, et al. Phenotypic Landscape
10 of Schizophrenia-Associated Genes Defines Candidates and Their Shared Functions. *Cell*.
11 2019;177:478–91.e20.

12 21. Liu K, Petree C, Requena T, Varshney P, Varshney GK. Expanding the CRISPR Toolbox in
13 Zebrafish for Studying Development and Disease. *Front Cell Dev Biol*. 2019;7:13.

14 22. Zischewski J, Fischer R, Bortesi L. Detection of on-target and off-target mutations generated
15 by CRISPR/Cas9 and other sequence-specific nucleases. *Biotechnol Adv*. 2017;35:95–104.

16 23. Zhu X, Xu Y, Yu S, Lu L, Ding M, Cheng J, et al. An efficient genotyping method for
17 genome-modified animals and human cells generated with CRISPR/Cas9 system. *Sci Rep*.
18 2014;4:6420.

19 24. Brocal I, White RJ, Dooley CM, Carruthers SN, Clark R, Hall A, et al. Efficient
20 identification of CRISPR/Cas9-induced insertions/deletions by direct germline screening in
21 zebrafish. *BMC Genomics*. 2016;17:259.

22 25. Liu G, Zhang Y, Zhang T. Computational approaches for effective CRISPR guide RNA
23 design and evaluation. *Comput Struct Biotechnol J*. 2020;18:35–44.

24 26. Moreno-Mateos MA, Vejnar CE, Beaudoin J-D, Fernandez JP, Mis EK, Khokha MK, et al.
25 CRISPRscan: designing highly efficient sgRNAs for CRISPR-Cas9 targeting in vivo. *Nat
26 Methods*. 2015;12:982–8.

27 27. Tsai SQ, Nguyen NT, Malagon-Lopez J, Topkar VV, Aryee MJ, Joung JK. CIRCLE-seq: a
28 highly sensitive in vitro screen for genome-wide CRISPR-Cas9 nuclease off-targets. *Nat
29 Methods*. 2017;14:607–14.

30 28. Tsai SQ, Zheng Z, Nguyen NT, Liebers M, Topkar VV, Thapar V, et al. GUIDE-seq enables
31 genome-wide profiling of off-target cleavage by CRISPR-Cas nucleases. *Nat Biotechnol*.
32 2015;33:187–97.

33 29. Mooney MR, Davis EE, Katsanis N. Analysis of Single Nucleotide Variants in CRISPR-
34 Cas9 Edited Zebrafish Exomes Shows No Evidence of Off-Target Inflation. *Front Genet*.
35 2019;10:949.

1 30. Iyer V, Boroviak K, Thomas M, Doe B, Riva L, Ryder E, et al. No unexpected CRISPR-
2 Cas9 off-target activity revealed by trio sequencing of gene-edited mice. *PLoS Genet.*
3 2018;14:e1007503.

4 31. Dong Y, Li H, Zhao L, Koopman P, Zhang F, Huang JX. Genome-Wide Off-Target Analysis
5 in CRISPR-Cas9 Modified Mice and Their Offspring. *G3* . 2019;9:3645–51.

6 32. Brinkman EK, Chen T, Amendola M, van Steensel B. Easy quantitative assessment of
7 genome editing by sequence trace decomposition. *Nucleic Acids Res.* 2014;42:e168.

8 33. Hsiau T, Conant D, Rossi N, Maures T, Waite K, Yang J, et al. Inference of CRISPR Edits
9 from Sanger Trace Data. doi:10.1101/251082.

10 34. Lindsay H, Burger A, Biyong B, Felker A, Hess C, Zaugg J, et al. CrispRVariants charts the
11 mutation spectrum of genome engineering experiments. *Nat Biotechnol.* 2016;34:701–2.

12 35. Montague TG, Cruz JM, Gagnon JA, Church GM, Valen E. CHOPCHOP: a CRISPR/Cas9
13 and TALEN web tool for genome editing. *Nucleic Acids Res.* 2014;42 Web Server issue:W401–
14 7.

15 36. Labun K, Montague TG, Krause M, Torres Cleuren YN, Tjeldnes H, Valen E. CHOPCHOP
16 v3: expanding the CRISPR web toolbox beyond genome editing. *Nucleic Acids Res.*
17 2019;47:W171–4.

18 37. Heigwer F, Kerr G, Boutros M. E-CRISP: fast CRISPR target site identification. *Nat
19 Methods.* 2014;11:122–3.

20 38. Xie X, Ma X, Zhu Q, Zeng D, Li G, Liu Y-G. CRISPR-GE: A Convenient Software Toolkit
21 for CRISPR-Based Genome Editing. *Mol Plant.* 2017;10:1246–9.

22 39. Hwang G-H, Park J, Lim K, Kim S, Yu J, Yu E, et al. Web-based design and analysis tools
23 for CRISPR base editing. *BMC Bioinformatics.* 2018;19:542.

24 40. Stemmer M, Thumberger T, Del Sol Keyer M, Wittbrodt J, Mateo JL. CCTop: An Intuitive,
25 Flexible and Reliable CRISPR/Cas9 Target Prediction Tool. *PLoS One.* 2015;10:e0124633.

26 41. LaFave MC, Varshney GK, Vemulapalli M, Mullikin JC, Burgess SM. A defined zebrafish
27 line for high-throughput genetics and genomics: NHGRI-1. *Genetics.* 2014;198:167–70.

28 42. Lazzarotto CR, Nguyen NT, Tang X, Malagon-Lopez J, Guo JA, Aryee MJ, et al. Defining
29 CRISPR-Cas9 genome-wide nuclease activities with CIRCLE-seq. *Nat Protoc.* 2018;13:2615–
30 42.

31 43. Chung C-H, Allen AG, Sullivan NT, Atkins A, Nonnemacher MR, Wigdahl B, et al. Computational
32 Analysis Concerning the Impact of DNA Accessibility on CRISPR-Cas9
33 Cleavage Efficiency. *Mol Ther.* 2020;28:19–28.

34 44. Doench JG, Fusi N, Sullender M, Hegde M, Vaimberg EW, Donovan KF, et al. Optimized

1 sgRNA design to maximize activity and minimize off-target effects of CRISPR-Cas9. *Nat*
2 *Biotechnol.* 2016;34:184–91.

3 45. Sundaresan R, Parameshwaran HP, Yugesha SD, Keilbarth MW, Rajan R. RNA-Independent
4 DNA Cleavage Activities of Cas9 and Cas12a. *Cell Rep.* 2017;21:3728–39.

5 46. Wimhurst JM, Manchester KL. Comparison of ability of Mg and Mn to activate the key
6 enzymes of glycolysis. *FEBS Lett.* 1972;27:321–6.

7 47. Coudray A, Battenhouse AM, Bucher P, Iyer VR. Detection and benchmarking of somatic
8 mutations in cancer genomes using RNA-seq data. *PeerJ.* 2018;6:e5362.

9 48. Sentmanat MF, Peters ST, Florian CP, Connelly JP, Pruett-Miller SM. A Survey of
10 Validation Strategies for CRISPR-Cas9 Editing. *Sci Rep.* 2018;8:888.

11 49. Suurväli J, Whiteley AR, Zheng Y, Gharbi K, Leptin M, Wiehe T. The Laboratory
12 Domestication of Zebrafish: From Diverse Populations to Inbred Substrains. *Mol Biol Evol.*
13 2020;37:1056–69.

14 50. Coe TS, Hamilton PB, Griffiths AM, Hodgson DJ, Wahab MA, Tyler CR. Genetic variation
15 in strains of zebrafish (*Danio rerio*) and the implications for ecotoxicology studies.
16 *Ecotoxicology.* 2009;18:144–50.

17 51. Westerfield M. The Zebrafish Book: A Guide for the Laboratory Use of Zebrafish (*Danio*
18 *Rerio*). 2007.

19 52. Quinlan AR. BEDTools: The Swiss-Army Tool for Genome Feature Analysis. *Curr Protoc*
20 *Bioinformatics.* 2014;47:11.12.1–34.

21 53. Van der Auwera GA, Carneiro MO, Hartl C, Poplin R, Del Angel G, Levy-Moonshine A, et
22 al. From FastQ data to high confidence variant calls: the Genome Analysis Toolkit best practices
23 pipeline. *Curr Protoc Bioinformatics.* 2013;43:11.10.1–11.10.33.

24 54. Jao L-E, Appel B, Wente SR. A zebrafish model of lethal congenital contracture syndrome 1
25 reveals Gle1 function in spinal neural precursor survival and motor axon arborization.
26 *Development.* 2012;139:1316–26.

27 55. Li H, Durbin R. Fast and accurate short read alignment with Burrows-Wheeler transform.
28 *Bioinformatics.* 2009;25:1754–60.

29 56. Schindelin J, Arganda-Carreras I, Frise E, Kaynig V, Longair M, Pietzsch T, et al. Fiji: an
30 open-source platform for biological-image analysis. *Nat Methods.* 2012;9:676–82.

31 57. Wu X, Kriz AJ, Sharp PA. Target specificity of the CRISPR-Cas9 system. *Quantitative*
32 *Biology.* 2014;2:59–70. doi:10.1007/s40484-014-0030-x.

33 58. Dobin A, Gingeras TR. Mapping RNA-seq Reads with STAR. *Curr Protoc Bioinformatics.*
34 2015;51:11.14.1–11.14.19.

1 59. McLaren W, Gil L, Hunt SE, Riat HS, Ritchie GRS, Thormann A, et al. The Ensembl
2 Variant Effect Predictor. *Genome Biol.* 2016;17:122.

3 60. Andrews S, Others. FastQC: a quality control tool for high throughput sequence data. 2010.

4 61. Bolger AM, Lohse M, Usadel B. Trimmomatic: a flexible trimmer for Illumina sequence
5 data. *Bioinformatics.* 2014;30:2114–20.

6 62. Patro R, Duggal G, Love MI, Irizarry RA, Kingsford C. Salmon provides fast and bias-aware
7 quantification of transcript expression. *Nat Methods.* 2017;14:417–9.

8 63. Love MI, Huber W, Anders S. Moderated estimation of fold change and dispersion for RNA-
9 seq data with DESeq2. *Genome Biol.* 2014;15:550.

10 64. Yu G, Wang L-G, Han Y, He Q-Y. clusterProfiler: an R package for comparing biological
11 themes among gene clusters. *OMICS.* 2012;16:284–7.

12 65. Zhou G, Soufan O, Ewald J, Hancock REW, Basu N, Xia J. NetworkAnalyst 3.0: a visual
13 analytics platform for comprehensive gene expression profiling and meta-analysis. *Nucleic
14 Acids Res.* 2019;47:W234–41.

15 66. Xia J, Gill EE, Hancock REW. NetworkAnalyst for statistical, visual and network-based
16 meta-analysis of gene expression data. *Nature Protocols.* 2015;10:823–44.
17 doi:10.1038/nprot.2015.052.

18 67. Team RC. R: A language and environment for statistical computing. 2017.

19 68. Larsson J. eulerr: area-proportional Euler and Venn diagrams with ellipses. R package
20 version. 2018;4.

21

22 **FIGURE LEGENDS**

23 **Figure 1. Workflow for the evaluation of CRISPR cleavages in NHGRI-1 zebrafish**
24 **embryos.** **(A)** The cartoon depicts our experiment, which included 50 gRNAs individually
25 microinjected into one-cell stage embryos, DNA extracted from 20 pooled G₀ larvae, and
26 genomic regions targeted by the gRNA amplified. Cartoon lightning symbols represent a
27 cleavage event. **(B)** An *in vivo* score was obtained from the Sanger sequencing traces using the
28 ICE and TIDE tools, with an example output from ICE pictured. **(C)** Scores for the two tools
29 were plotted with values below the median in orange and above the median in purple. **(D)** Scores

1 from ICE and TIDE tools were compared for a subset of six gRNAs compared to mosaicism
2 percentages from Illumina sequencing of the same region. **(D)** From the PAGE, an empirical
3 intensity ratio was obtained and compared to the *in vivo* efficiency scores. Spearman correlations
4 results are shown in the scatter plots with the line of best fit included.

5

6 **Figure 2. Correlation of on-target efficiencies calculated using different methods.** Scores
7 from *in silico* prediction tools, an *in vitro* protocol [27], and cutting cleavages obtained *in vivo*
8 using a deconvolution tool [33] for 50 gRNAs were compared using Spearman correlations. Each
9 box includes the correlation result with the *p-value* in parenthesis. The color of the boxes
10 represent the correlation values , ranging between -1 (blue) and 1 (red).

11

12 **Figure 3. Assessment of off-target cleavage events using different prediction methods.** **(A)**
13 The number of predicted CRISPRScan off-target sites correlated with the number of identified
14 CIRCLE-seq sites (Spearman correlation). Log normalization was used to reduce the range in the
15 number of sites. **(B)** *In vivo* editing scores from the ICE tool for the top predicted off-target sites
16 using CRISPRScan and CIRCLE-seq were not different. Scores were compared using a Mann-
17 Whitney U test. **(C)** Editing efficiencies at predicted off-target sites using *in vivo* scores from
18 Sanger sequencing and mosaicism % from Illumina sequencing were correlated (Spearman
19 correlation). **(D)** Editing scores obtained *in vivo* at off-target sites were not correlated with the
20 on-target efficiency of the gRNA. All scatter plots include the Spearman correlations results with
21 the line of best fit.

22

23 **Figure 4. Evaluation of spurious genomic mutations in CRISPR-injection controls.** **(A)** The

1 abundance of protein-coding genes carrying frameshift variants for each Cas9-injected treatment
2 are depicted in a Venn diagram, with mutated genes identified in both treatments listed. **(B)**
3 Genomic DNA from zebrafish larvae injected with Cas9 enzyme, Cas9 mRNA, catalytically
4 dead Cas9 (dCas9), a scrambled gRNA, uninjected batch siblings, and a fin clip from their
5 parents was used to perform targeted Illumina sequencing of 21 genes to quantify indel
6 mosaicism with average \pm standard deviation values listed in the table (see Supplementary Table
7 1 and Supplementary Table 7 for the description of the genes).

8

9 **Figure 5. Evaluation of expression variability in CRISPR-injection controls.** **(A)** Principal
10 components analysis using the transcript abundances in larvae injected with Cas9 enzyme (Enz1,
11 Enz2, Enz3), Cas9 mRNA (RNA1, RNA2, RNA3), uninjected siblings (Uni1, Uni2), and
12 uninjected siblings from a different batch (Uni3, Uni4, Uni5). **(B)** Volcano plots show the
13 differentially-expressed genes in Cas9-enzyme and Cas9-mRNA injected larvae with the number
14 (and %) of upregulated (fold change > 1) and downregulated (fold change < -1) genes. The top
15 five representative up- and downregulated genes are highlighted, with the full list of genes
16 available as Supplementary Table 6. **(C)** Differentially-expressed genes across samples injected
17 with Cas9 enzyme or Cas9 mRNA relative to uninjected batch-siblings show significant
18 correlations. Plots include the numbers and percentages (in parentheses) of genes downregulated
19 (blue) and upregulated (red) in both Cas9 treatments from the total amount of genes assayed (n=
20 30,258).